A Unique Approach to the Mobile Proton Model: Influence of Charge Distribution on Peptide Fragmentation

Feng Sun,[†] Rutao Liu,*[,†] Wansong Zong,[†] Yanmin Tian, Meijie Wang, and Pengjun Zhang

School of Environmental Science and Engineering, Shandong University, 27 Shanda South Road, Jinan 250100, P. R. China

Received: December 13, 2009

The cleavage processes of protonated peptides in mass spectrometry, described in the mobile proton model, are charge-directed and depend on the charge distribution around the cleavage sites. Previous studies experimentally verified the mobile proton model by changing peptide sequences. In this study, oxidation was applied to change the charge distribution of peptides, but the sequence was retained. Tandem mass spectrometry (MS/MS) and quantum chemical calculations at the B3LYP/6-31G(d) level were used to test the validity of the mobile proton model. The results showed prominent differences of peptide fragmentation efficiency caused by the charge distribution produced by various oxidation levels. Fragmentation efficiency curves coupled with the relative intensities of the fragments indicated that the cleavage of the peptide Ala-Arg-Arg-Ala (ARRA) became more and more difficult as O atoms were added. The relative charge ratios between C and N atoms in the amide bonds decreased with the increase of oxidation extent, suggesting that oxidation resulted in protons moving away from the amide bonds. The combined methods proposed here provide a unique approach to substantiate and refine the mobile proton model for peptide fragmentation.

Introduction

Peptide fragmentation analysis in tandem mass spectrometry (MS/MS) has become a powerful technique for peptide and protein identification.[1−3] The sequence of target peptides can be determined by comparing the MS/MS data with theoretical fragmentation patterns. However, the existing database is limited to explaining the various intensities of fragmentation ions.[3−7] Clarifying the selective cleavage mechanism of peptides can provide a theoretical basis for peptide identification.

The mobile proton model is a major cleavage theory for peptides. It claims that the cleavage processes of protonated peptides are charge-directed, and the proton in a more basic region can transfer to the amide nitrogen atoms (the main cleavage site) after it is given some energy, producing b_n ions, y_n ions, and so forth.[4,8,9] This theory has been supported by experiments on the cleavage mechanism of peptides using fragmentation efficiency curves[5,8,10] or quantum chemistry calculations.[11−13] Fragmentation efficiency curves can be used to measure how easily peptide fragments and the results show that the cleavage process of protonated peptides depends on the number of added protons, peptide composition, gas-phase basicity, and chemical modification.[5,8,10] But, in these studies the sequences of peptides were changed, which led to significant differences from the process described in the mobile proton model. Quantum chemistry studies on the peptide cleavage process have shown that the protonated amide nitrogen atoms activate the cleavage of charge-induced MS fragment ions.[4,14] However, they did not include the charge distribution on the peptides in the cleavage process, which can neither explain the selective cleavage of peptides in low energy MS nor predict the relative intensities of the corresponding fragment ions. So, exploring the cleavage and charge distribution of peptides without changing the sequence will substantiate and refine the mobile proton model.

Arginine-containing peptides provide a strong signal in positive ion electrospray ionization mass spectrometry (ESI-MS; the pK_a of Arg is about 12.5) and are always used as model peptides.[15−21] The oxidation of Arg, which is expected to be quite susceptible to attack by hydroxyl radicals, will significantly change the charge distribution of Arg-containing peptides without necessitating a change of peptide sequence, as in previous studies. In this paper, a simple model peptide containing two arginine residues, Ala-Arg-Arg-Ala, was selected for radiolytic oxidation and analysis to explore its selective cleavage mechanism. MS and MS/MS were used to identify the oxidation products and the corresponding oxidation sites, respectively. Combining the fragmentation energy curves and the relative intensities of fragment ions, the influence of oxidation on the cleavage of ARRA was studied. Moreover, MS/MS data and charge distribution obtained by quantum chemical calculations at the B3LYP/6-31G(d) level of theory were incorporated to provide reasonable evidence for the mobile proton model.

Experimental Procedures

Materials. The peptide Ala-Arg-Arg-Ala (ARRA) was purchased from GL Biochem Inc. (Shanghai, China), and had a purity at least of 95%. Thiourea and trifluoroacetic acid (TFA) were ordered from Sinopharm Chemical Reagent Inc. (Shanghai, China). High-performance liquid chromatography (HPLC) acetonitrile was purchased from Merck (Germany). Solutions of peptide at a concentration of 40 μM were prepared with ultrapure water from a Millipore Ultrapure water system.

Oxidation of Model Peptide. The peptide solution was exposed to a cobalt-60 γ-ray source (5 Gy/min) at the Agricultural Sciences Academy of Shandong Province. For 40 μM ARRA, 600 μL of the solution in a 1.5 mL Eppendorf tube was exposed for 2 min. After exposure to radiation, 30 μL of

* To whom correspondence should be addressed. Phone/Fax: 86-531-88364868. E-mail: rutaoliu@sdu.edu.cn.

† These authors made equal contributions to this work and share the first authorship.

10.1021/jp911772q
Published on Web 04/23/2010

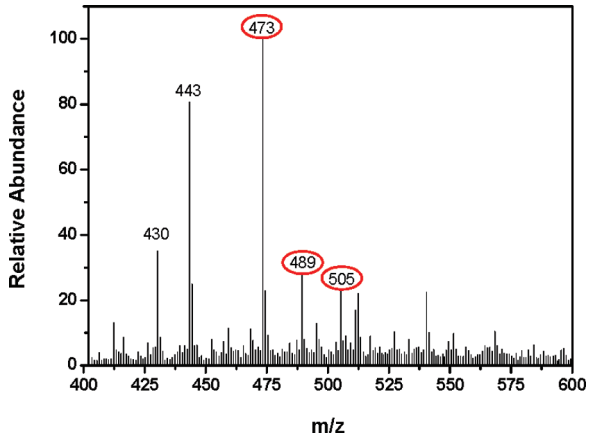

Figure 1. Positive ESI mass spectrum of ARRA exposed to γ-rays for 2 min.

thiourea (0.2 M) was added into the Eppendorf tube to eliminate the surviving oxidants, and finally the sample was stored at 0−4 °C before MS analysis.

Mass Spectrometric Analysis. The radiolytically oxidized and unoxidized peptides were analyzed directly by ESI-MS without chromatographic separation. The concentration was adjusted to 20 μM with acetonitrile (containing 0.1% TFA) and was infused directly into the ESI-MS at a flow rate of 3 μL/min. Mass spectra were acquired on a LCQ Fleet mass spectrometer (ThermoFisher). The protonated peptides were formed by ESI. The ESI source conditions were set as follows: needle voltage 3500 V, sample cone voltage 55 V, extraction cone voltage 0.5 V, source temperature 110 °C, and cone gas (N_2) 30 L/h. The instrument was tuned using a known mass of the unmodified peptide ARRA (472). To determine the sites of amino acid oxidation, the collision-induced dissociation (CID) MS/MS spectra were acquired for total ion chromatogram (TIC).

Quantum Chemical Calculations. All of the charge distribution results reported in this paper were calculated at the B3LYP level of theory using the Gaussian 03W program. A 6-31G(d) basis set has been implemented to perform efficient, yet accurate, calculations. The fully optimized ARRA molecular structure was obtained through minimum-energy geometry optimizations. Calculations of electronic and structural properties allow direct comparisons with experimental measurements, including the analysis of charge distribution.

Results and Discussion

Radiolytic Oxidation Sites of ARRA. The molecular ion of the unmodified peptide has a peak at *m/z* 473 in the positive ESI-MS spectrum of ARRA (Figure 1). Compared with the native peptide, the two oxidation products with one (*m/z* 489) or two (*m/z* 505) oxygen atoms added have different charge distributions but uniform sequences.

To identify the oxidation sites of ARRA with oxygen atoms added, we analyzed the tandem mass spectra of model peptide and its oxidation products using CID. It can be seen from Figure 2A that the fragmentation ions of ARRA include various b_n and y_n types, which are generated by the cleavage of the amide bonds within the peptide. The MS/MS spectrum of ion *m/z* 489

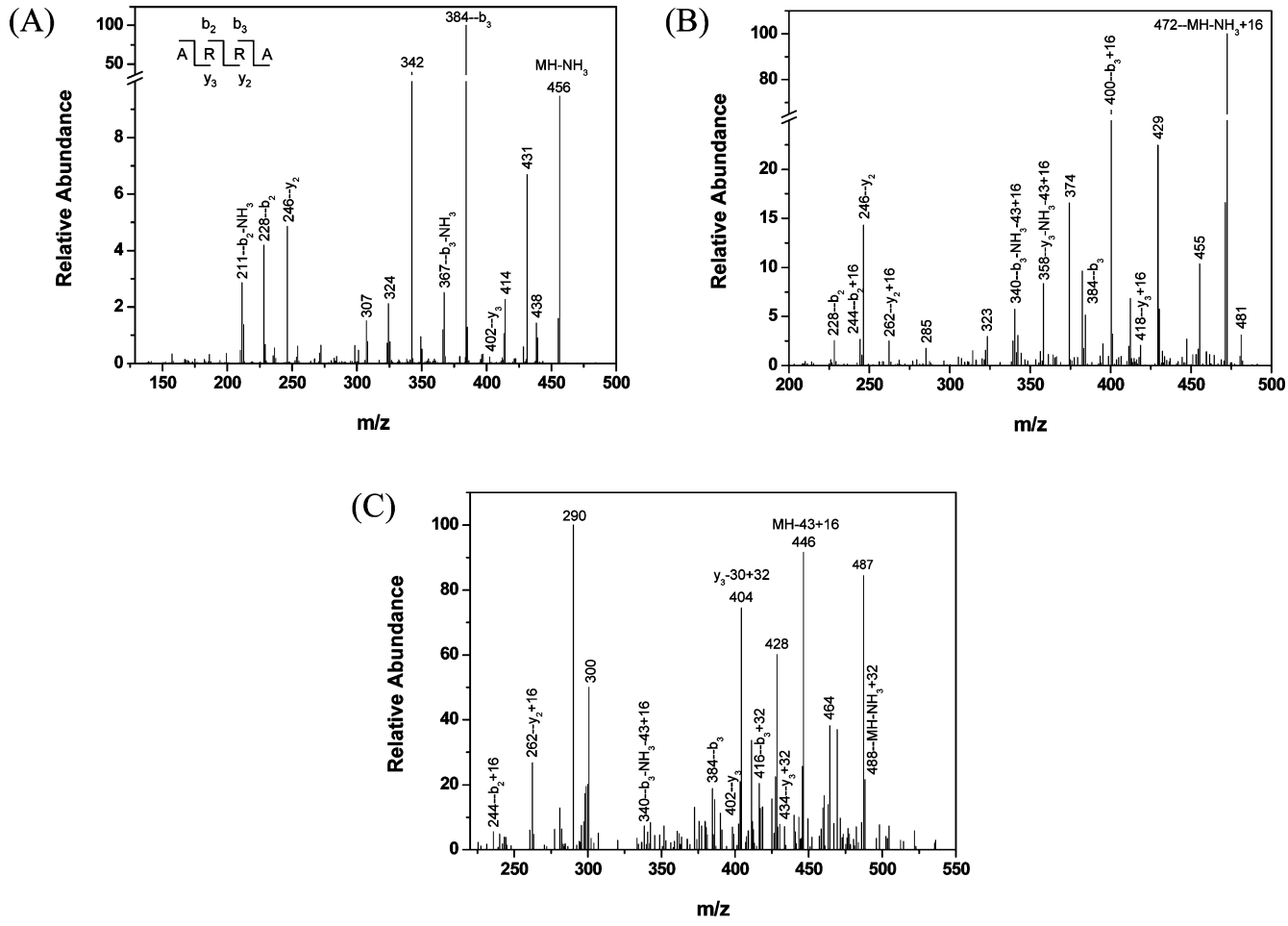

Figure 2. MS/MS spectra of ion at *m/z* (A) 473 (model peptide), (B) 489 (+16 Da), and (C) 505 (+32 Da) with collision energy at 35 eV.

SCHEME 1: Proposed Mechanism for Formation of +16 Da Oxidation Product from an Arginine Residue

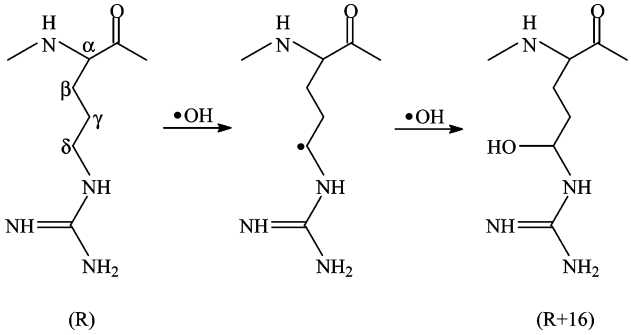

SCHEME 2: Structure of ARRA: Amide Bonds 1, 2, and 3 Referred to below

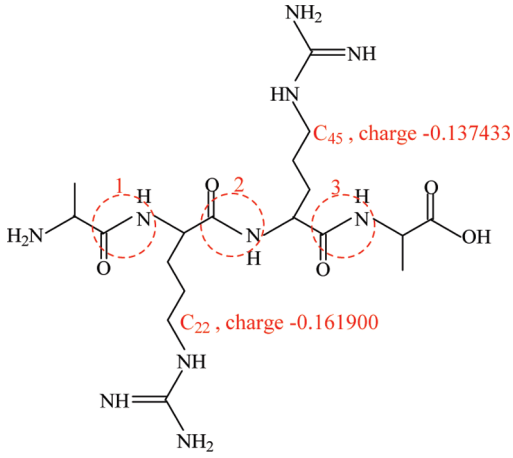

(Figure 2B) revealed that either arginine residue could be oxidized because the 16 Da additional mass was detected on the b_2, y_2, b_3, and y_3 fragment ions. However, the oxidation degree of the b_2 ion is clearly higher than that of the y_2 ion, suggesting the Arg residue close to the N-terminal side of the peptide is the main oxidation site. Comparing the MS/MS spectra of ARRA (Figure 2A) and its oxidation product with two O atoms added (Figure 2C), we find that a shift of +16 Da can be detected for b_2 and y_2 fragment ions, while the +32 Da is only detected for b_3 and y_3 fragment ions, which indicates the two O atoms are located on different arginine residues.

In the oxidation of arginine, it has been reported that the O atom is mainly incorporated into δ-CH_2 among all methylene side-chain carbons.[22] The mechanism of arginine oxidation for the formation of the +16 Da product is presented in Scheme 1. A hydroxyl radical abstracts a hydrogen from the δ-carbon of the side chain and adds a hydroxyl group to form an intermediate oxidation product with +16 Da mass, as compared to the parent arginine residue.

We also found that the two δ-CH_2 (C_{22} and C_{45}) of arginine side chains in ARRA (Scheme 2) showed different activities to •OH calculated at the B3LYP/6-31G(d) level. Results show that C_{22} has a bigger negative charge and is the major oxidation site of ARRA (consistent with the results in Figure 2B).

Fragmentation Efficiency Curves for Native and Oxidized ARRA. Fragmentation efficiency curves are obtained by plotting fragmentation data (∑(fragment ion intensity)/∑(total ion intensity)) versus collision energy. In Figure 3, fragmentation efficiency curves are illustrated to represent peptides with or without oxidation. The relatively steep slope of the curve shows a dramatic change in the extent of peptide fragmentation.

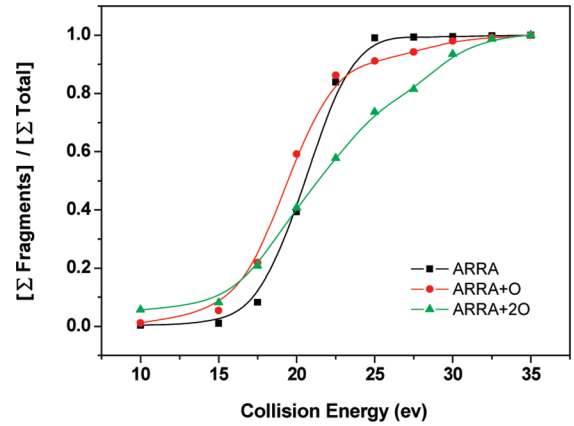

Figure 3. Fragmentation efficiency curves of MH^+ ions (ESI) for ARRA and its oxidation products. The *y* axis represents ∑(fragment ion intensity)/∑(total ion intensity), and the *x* axis represents CID collison energy.

TABLE 1: Relative Intensities of b_n and y_n Ions in the Native and Oxidized ARRA[a,b]

fragment ions	MH	MH + O	MH + 2O
$b_2 - NH_3$	78.90552	1.592378	1.557468
b_2	141.1059	8.311387	1.3011
$b_2 + H_2O$	260.4183	34.385196	5.435519
$y_2 - NH_3$	30.66252	2.122925	ND
y_2	260.4183	34.385196	5.435519
$b_3 - NH_3$	103.1628	8.519356	ND
b_3	6276.348	255.59695	8.72254
$b_3 + H_2O$	12.64656	9.230607	3.990833
$y_3 - NH_3$	36.82712	5.020637	2.503744
y_3	12.64656	9.230607	3.990833

[a] MH stands for the protonated peptide of ARRA. [b] ND = not detected.

Compared with the native peptide, the fragmentation efficiency curves of the oxidized peptides have slower fragmentation trends as the extent of oxidation increases. Therefore, the more oxygen atoms appear in ARRA, the more difficult fragmentation of the corresponding peptide becomes.

Relative Intensities of b_n and y_n Ions. The cleavage extent of peptides can also be measured by analyzing the relative intensities of b_n and y_n ions. The relative fragment intensities obtained at 25 eV collision energy (calculated by setting the intensity of parent peptide ions as 100) of the peptides oxidized to different extents are listed in Table 1. The relative intensity of each fragment ion tends to decrease with the increase of oxidation extent, indicating that cleavage is more difficult to achieve because of the oxidation (consistent with the results of the fragmentation efficiency curves).

Relationship between Charge Distribution and Fragmentation. Recent studies using quantum chemical calculations at the B3LYP/6-31G(d) level[14,23,24] have led us to believe that this level of theory can give consistently reliable conformationally dependent charges and energies for peptides. The charge distribution on the amide bonds (Table 2) can provide a way to explore peptide fragmentation. To find the change of charge distribution after the oxidation of ARRA, a simple comparison of the relative charge on the C and N atoms (Q_C/Q_N) in the amide bonds is listed in Table 3. The relative charges mostly decrease. The only increases occur when the oxidation site is C_{45}, which is close to the C-terminal side of the peptide. As previously concluded, C_{22} is the major oxidation site of ARRA. Therefore, the main trend is toward a decreased relative charge

TABLE 2: Charge Distribution of Amide Bonds[a,b]

	protonated at the arginine close to the C-terminal side				protonated at the arginine close to the N-terminal side			
		MH + O				MH + O		
	MH	(C_{45} + O)	(C_{22} + O)	MH + 2O	MH	(C_{45} + O)	(C_{22} + O)	MH + 2O
1 Q_C	0.61737	0.61716	0.61785	0.61785	0.61884	0.61892	0.61921	0.61963
1 Q_N	−0.62057	−0.62044	−0.62008	−0.62003	−0.62977	−0.62962	−0.62951	−0.62973
2 Q_C	0.59804	0.59745	0.59820	0.59767	0.59769	0.59720	0.59782	0.59771
2 Q_N	−0.60204	−0.59999	−0.60135	−0.59939	−0.59050	−0.58836	−0.58996	−0.58795
3 Q_C	0.63330	0.63359	0.63338	0.63395	0.63246	0.63274	0.63267	0.63270
3 Q_N	−0.61447	−0.61496	−0.61415	−0.61459	−0.61844	−0.61888	−0.61828	−0.61825
1 Q_C/Q_N	−0.99484	−0.99471	−0.99640	−0.99648	−0.98264	−0.98301	−0.98364	−0.98396
2 Q_C/Q_N	−0.99336	−0.99577	−0.99476	−0.99713	−1.01218	−1.01503	−1.01332	−1.0166
3 Q_C/Q_N	−1.03064	−1.03030	−1.03131	−1.03150	−1.02267	−1.02240	−1.02327	−1.02337

[a] MH stands for the protonated peptide of ARRA. [b] 1, 2, and 3 stand for the three amide bonds marked in Scheme 2.

TABLE 3: Relative Charge Comparison between C and N Atoms in the Amide Bonds[a,b]

	protonated at the arginine close to the C-terminal side				protonated at the arginine close to the N-terminal side			
		MH + O				MH + O		
	MH	(C_{45} + O)	(C_{22} + O)	MH + 2O	MH	(C_{45} + O)	(C_{22} + O)	MH + 2O
1 Q_C/Q_N	-	↑	↓	↓↓	-	↓	↓	↓↓
2 Q_C/Q_N	-	↓	↓	↓↓	-	↓	↓	↓↓
3 Q_C/Q_N	-	↑	↓	↓↓	-	↑	↓	↓↓

[a] MH stands for the protonated peptide of ARRA. [b] 1, 2, and 3 stand for the three amide bonds marked in Scheme 2. -: standard. ↑: increased. ↓: decreased. ↓↓: further decreased.

of the amide bonds oxidized at C_{22}. When the extent of oxidation is increased (with two O atoms separately added at C_{22} and C_{45}), the decreased charge is even more apparent. This phenomenon shows that the oxidation weakens the basicity of the arginine residue, decreasing the proton transfer to the amide bonds; thus the oxidized peptides fragment is less than the unoxidized ones. In the mobile proton model, the protons are expected to move to the amide bond away from basic sites, so by directly lowering the basicity through oxidation, we can confirm the model's predictions experimentally.

Conclusions

The mobile proton model, supported by MS/MS results and quantum chemical calculations, possesses a central role in evaluating the influence of charge distribution on peptide fragmentation. According to the experimental results, the oxidation of ARRA is limited to C_{22} and C_{45}. The major oxidation site of +16 Da products is C_{22}, while for the +32 Da products, O atoms cannot be located on the same Arg residue but are separately added at C_{22} and C_{45}. With the O atoms added, the cleavage of ARRA becomes more difficult. The charge distribution obtained by quantum chemical calculations at the B3LYP/6-31G(d) level shows that the decrease of the relative charge ratio between C and N atoms in the amide bonds leads to a lower fragmentation efficiency of ARRA, as predicted by the model. The results described in this paper provide a distinct experimental basis to further substantiate and refine the mobile proton model for peptide dissociation by tandem mass spectrometry. We have experimental evidence for the influence of charge distribution on peptide fragmentation efficiency in peptides with the same sequence.

Acknowledgment. This work is supported by NSFC (20607011, 20875055), the Fok Ying Tong Education Foundation (111082), NCET-06-0582, and the Foundation for SRF for ROCS, SEM, Middle Young Scientists and Key Science-Technology Project in Shandong Province (2007BS08005, 2008GG10006012). The authors thank Dr. Pamela Holt for editing the manuscript.

References and Notes

(1) Kondo, T.; Sawa, S.; Kinoshita, A.; Mizuno, S.; Kakimoto, T.; Fukuda, H.; Sakagami, Y. *Science* **2006**, *313*, 845.
(2) Lu, B.; Motoyama, A.; Ruse, C.; Venable, J.; Yates, J. R. *Anal. Chem.* **2008**, *80*, 2018.
(3) Xu, G. Z.; Liu, R. T.; Zak, O.; Aisen, P.; Chance, M. R. *Mol. Cell. Proteomics* **2005**, *4*, 1959.
(4) Zhang, Z. Q. *Anal. Chem.* **2004**, *76*, 3908.
(5) Wysocki, V. H.; Tsaprailis, G.; Smith, L. L.; Breci, L. A. *J. Mass Spectrom.* **2002**, *35*, 1399.
(6) Sekiya, S.; Wada, Y.; Tanaka, K. *Anal. Chem.* **2004**, *76*, 5894.
(7) Fu, Q.; Li, L. J. *Rapid Commun. Mass Spectrom.* **2006**, *20*, 553.
(8) Dongre, A. R.; Jones, J. L.; Somogyi, A.; Wysocki, V. H. *J. Am. Chem. Soc.* **1996**, *118*, 8365.
(9) Dongre, A. R.; Somogyi, A.; Wysocki, V. H. *J. Mass Spectrom.* **1996**, *31*, 339.
(10) Jones, J. L.; Dongré, A. R.; Somogyi, A.; Wysocki, V. H. *J. Am. Chem. Soc.* **1994**, *116*, 8368.
(11) Madine, J.; Jack, E.; Stockley, P. G.; Radford, S. E.; Serpell, L. C.; Middleton, D. A. *J. Am. Chem. Soc.* **2008**, *130*, 14990.
(12) Madani, F.; Lind, J.; Damberg, P.; Adams, S. R.; Tsien, R. Y.; Gräslund, A. O. *J. Am. Chem. Soc.* **2009**, *131*, 4613.
(13) Hyun, S.; Kim, H. J.; Lee, N. J.; Lee, K. H.; Lee, Y.; Ahn, D. R.; Kim, K.; Jeong, S.; Yu, J. *J. Am. Chem. Soc.* **2007**, *129*, 4514.
(14) Paizs, B.; Léndvay, G.; Vekey, K.; Suhai, S. *Rapid Commun. Mass Spectrom.* **1999**, *13*, 525.
(15) Amici, A.; Levine, R. L.; Tsai, L.; Stadtman, E. R. *J. Biol. Chem.* **1989**, *264*, 3341.
(16) Climent, I.; Tsai, L.; Levine, R. L. *Anal. Biochem.* **1989**, *182*, 226.
(17) Ayala, A.; Cutler, R. G. *Free Radical Biol. Med.* **1996**, *21*, 65.
(18) Touboul, D.; Jecklin, M. C.; Zenobi, R. *J. Phys. Chem. B* **2007**, *111*, 11629.
(19) Pietzsch, J. *Biochem. Biophys. Res. Commun.* **2000**, *270*, 852.
(20) Pietzsch, J.; Julius, U. *FEBS Lett.* **2001**, *491*, 123.
(21) Requena, J. R.; Chao, C. C.; Levine, R. L.; Stadtman, E. R. *Proc. Natl. Acad. Sci. U.S.A.* **2001**, *98*, 69.
(22) Xu, G. Z.; Takamoto, K.; Chance, M. R. *Anal. Chem.* **2003**, *75*, 6995.
(23) Paizs, B.; Csonka, I. P.; Lendvay, G.; Suhai, S. *Rapid Commun. Mass Spectrom.* **2001**, *15*, 637.
(24) Csonka, I. P.; Paizs, B.; Lendvay, G.; Suhai, S. *Rapid Commun. Mass Spectrom.* **2001**, *15*, 1457.

JP911772Q